Proceedings of the Institution of Civil Engineers
Water & Maritime Engineering 154
September 2002 Issue 3
Pages 159–168

Paper 12154
Received 15/09/1999
Accepted 18/10/2001

Keywords:
hydraulics & hydrodynamics/mathematical modelling/coastal engineering





N. Christakis
Senior Research Fellow, School of Computing and Mathematical Sciences, Maritime Greenwich University Campus

N. W. H. Allsop
Manager, Coastal Structures Section, HR Wallingford

R. G. Beale
Senior Lecturer, Centre for Civil Engineering, Oxford Brookes University

A. J. Cooper
Principal Scientist, Ports and Estuaries Group, HR Wallingford

J. M. Dennis
Principal Lecturer, Centre for Civil Engineering, Oxford Brookes University

A volume of fluid numerical model for wave impacts at coastal structures

N. Christakis, N. W. H. Allsop, R. G. Beale, A. J. Cooper and J. M. Dennis

The first stages in the development of a new design tool, to be used by coastal engineers to improve the efficiency, analysis, design, management and operation of a wide range of coastal and harbour structures, are described. The tool is based on a two-dimensional numerical model, NEWMOTICS-2D, using the volume of fluid (VOF) method, which permits the rapid calculation of wave hydrodynamics at impermeable natural and man-made structures. The critical hydrodynamic flow processes and forces are identified together with the equations that describe these key processes. The different possible numerical approaches for the solution of these equations, and the types of numerical models currently available, are examined and assessed. Preliminary tests of the model, using comparisons with results from a series of hydraulic model test cases, are described. The results of these tests demonstrate that the VOF approach is particularly appropriate for the simulation of the dynamics of waves at coastal structures because of its flexibility in representing the complex free surfaces encountered during wave impact and breaking. The further programme of work, required to develop the existing model into a tool for use in routine engineering design, is outlined.

1. INTRODUCTION

The present design methods used to determine hydrodynamic loadings on breakwaters, quays, sea walls, embankments and related shoreline structures rely on simplistic empirical formulae or site-specific physical model tests. The empirical models available suffer from a number of significant limitations. They may predict simple responses, such as wave run-up, overtopping and reflections, and wave forces, but they are valid only for limited hydraulic conditions and structure geometries. Difficulties arise in the use of scale models where the particular response is influenced significantly by scale effects, as in the prediction of impact pressures on walls or embankments, or flows over or around such structures. A new design method, based on an advanced numerical model, is described that will permit the rapid calculation of wave hydrodynamics at natural and artificial structures. The model will enable wave–structure interactions to be determined.

A detailed description of the flow processes is required to allow design calculations of wave-induced flows and pressures near, at and within, porous and non-porous structures. Simple one-dimensional depth-averaged models have already been developed to calculate flows and pressures at and in rubble mounds, but the models are too limited for use in design studies. A more complex series of two-dimensional models, using boundary element techniques has also been developed, but these models are still unable to calculate complex flows at wave impact on a structure element. This paper describes the first stages in the development of two-dimensional models of wave action on the outer surface and within coastal structures, with the objective of obtaining a better understanding of flows at breakwaters and sea walls, and hence to develop improved design methods for coastal and shoreline structures.

2. REVIEW OF PAST WORK

Our understanding of breaking waves is limited due to a number of factors. These include the difficulties associated with obtaining experimental data and the limitations of existing computational models, such as the oversimplification of the interaction with structures and the restrictions associated with free surface modelling techniques. The simplest models assume that wave action may be described by the non-linear shallow water (NLSW) equations where flows may be averaged over water depth. NLSW models have been shown to accurately predict wave heights and depth-averaged velocities on structures and beaches, and have been used successfully to model run-up and overturning.[1–4] One-dimensional models are unable to provide detailed information about the flow regime throughout the depth of a wave and cannot be used to accurately predict impact forces, particularly whenever vertical accelerations exceed horizontal ones.

Two-dimensional models based on more comprehensive hydrodynamic models can overcome this limitation, and can calculate variations of velocity and pressure throughout the wave. Boundary element models (BEM) and boundary integral models (BIM) have been developed by several authors, such as Maiti and Sen,[5] Yasuda *et al.*,[6] and Grilli *et al.*[7] These methods rely on applying Green's theorem to Laplace's equation. However, these methods, while successfully enabling wave motions up to, and including, breaking to be analysed, are unable to simulate the full process of wave overturning as the method breaks down when particles collide and the region becomes multi-connected. Hence, these methods cannot be applied to problems of coastal structures where analyses of pressures and flow hydrodynamics after wave overturning and impact are required.

To analyse flows after wave overturning Harlow and Welsh[8] developed the pioneering Marker and Cell (MAC) method which models free surface flows by tracking the fluid interface through the motion of massless particles in the fluid rather than defining the free surface directly. The particles are used to determine the status of computational cells as either 'full', 'empty' or 'partially full' (i.e. surface cells). They do not affect the flow. Significant storage, particularly in three dimensions or for higher resolutions, is required to store all the markers. Hirt, Nichols and co-workers in a series of papers between 1979 and 1985[9–12] built the pioneering code SOLA-VOF and NASA-SOLA-VOF based on the volume of fluid (VOF) method at the Los Alamos National Laboratory, New Mexico, USA. The VOF method combines a discretisation of the Navier–Stokes equations and the use of a VOF function *F*, where *F* is the fractional VOF in a cell, to determine the position of the free surface. The *F* function is either 1 if the cell is full or 0 if the cell is empty, and between 0 and 1 for a surface cell which is partially full. The original SOLA-VOF code was used to study the propagation of shock waves from deep ocean earthquakes.[10] Since then, Hirt has produced a state-of-the-art program, FLOW 3D,[13] which includes non-uniform two-dimensional and three-dimensional meshes, fluid compressibility and complex boundaries in Cartesian and cylindrical coordinate systems.

Delft Hydraulics have developed a two-dimensional version of the SOLA-VOF called SKYLLA.[14,15] SKYLLA solves the Navier–Stokes equations by use of the Poisson equation for pressure in conjunction with the conjugate gradient algorithm. The program also incorporates the use of a weakly-reflective boundary. Bradford[16] used the VOF technique to investigate the effects of turbulence in the surf zone. The papers by Van Gent and Petit,[17] Bracci Laudiero (working with an early version of NEWMOTICS),[18] Troch and de Rouk,[19] and Liu *et al.*[20] describe the use of modified Navier–Stokes equations to analyse the flow in and around permeable structures, such as breakwaters.

3. THE DEVELOPMENT OF THE NEWMOTICS-2D VOF MODEL

Sabeur *et al.*[21] decided to develop their own version of the VOF code called NEWMOTICS-2D. This code was based on a discretised version of the two-dimesional Navier–Stokes and continuity equations. The Navier–Stokes equations were first discretised in time to give

$$\frac{u^{n+1}-u^n}{\delta t}+u^n\cdot\frac{\partial u^n}{\partial x}+v^n\cdot\frac{\partial u^n}{\partial y}=-\frac{\partial P^{n+1}}{\partial x}+\nu\nabla^2 u^n+g_x \quad (1)$$

$$\frac{v^{n+1}-v^n}{\delta t}+u^n\cdot\frac{\partial v^n}{\partial x}+v^n\cdot\frac{\partial v^n}{\partial y}=-\frac{\partial P^{n+1}}{\partial y}+\nu\nabla^2 v^n+g_y \quad (2)$$

followed by a discretisation in space. This produces

$$u^{n+1}_{i+1,j}+\delta t\cdot\frac{P^{n+1}_{i+1,j}-P^{n+1}_{i,j}}{\delta x}=u^n_{ij}+\delta t\cdot A^n_{ij} \quad (3)$$

$$v^{n+1}_{1,j+1}+\delta t\cdot\frac{P^{n+1}_{i,j-1}-P^{n+1}_{i,j}}{\delta y}=v^n_{ij}+\delta t\cdot B^n_{ij} \quad (4)$$

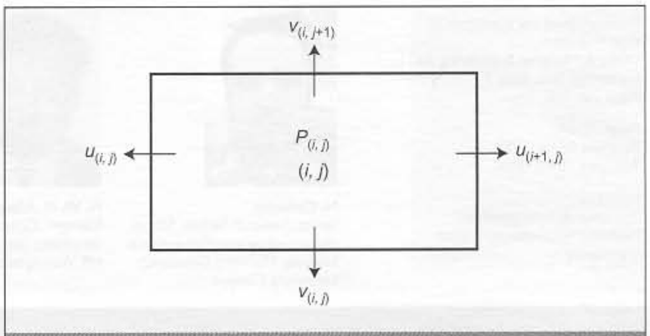

Fig. 1. A typical cell (*i*, *j*) in NEWMOTICS-2D (note that all velocity components are taken at the cell faces, while the pressure is taken at the centre of the cell)

A and *B* are finite difference operators involving the discretisation of the non-linear and diffusion terms and the external fields that appear within the Navier–Stokes equations. *u* and *v* are the velocities in the *x* and *y* spatial directions. $P^{n+1}_{i,j}$ is the pressure at the centre of cell i, j at time-step $n+1$. The Poisson equation can be finally derived by combining equations (3) and (4) with the equation of continuity to give

$$\frac{P^{n+1}_{i+1,j}-2P^{n+1}_{i,j}+P^{n+1}_{i-1,j}}{\delta x^2}+\frac{P^{n+1}_{i,j+1}-2P^{n+1}_{i,j}+P^{n+1}_{i,j-1}}{\delta y^2}=\frac{A^n_{i,j}-A^n_{i-1,j}}{\delta x}+\frac{B^n_{i,j}-B^n_{i,j-1}}{\delta y} \quad (5)$$

Note that pressures and body forces are discretised at the centre of a cell and velocities on the mid-sides of cell boundaries. A typical model cell can be seen in Fig. 1.

The boundary conditions used by Sabeur *et al.*[21] were normal velocities parallel to boundaries with the gradient of the tangential velocities set to zero. Parallel (or anti-parallel) and equal in magnitude virtual velocities are set for free-slip (or no-slip) conditions. These conditions were easy to implement for horizontal and vertical boundaries. For inclined boundaries, two different approaches were used. Firstly, for an inclined bed the whole grid was inclined to be parallel to the bed surface. Secondly, for a sloping structure the surface was represented as a series of steps. In this case, the Poisson equation could be derived for each separate step.

The boundary equations for a free surface are different from those at solid boundaries. They depend on the accurate evaluation of the *F* function and its local gradients at neighbouring cells to the free surface cell involved in the computation. The *F* function defining the free surface must satisfy the transport equation

$$\frac{\partial F}{\partial t}+u\frac{\partial F}{\partial x}+v\frac{\partial F}{\partial y}=0 \quad (6)$$

The free surface is advected either horizontally or vertically, the direction being that which is most normal to the free surface. The surface cell pressure P_{ij} was calculated by interpolating the desired pressure P_s at the interface from the inside pressure of the interpolation cell $(i-1, j)$

$$P_{ij}=(1-\kappa)\cdot P_{i-1,j}+\kappa\cdot P_s \quad (7)$$

where κ is the ratio of the distance between the centre of the cells $(i-1, j)$ and (i, j) to the distance between the free surface point and the centre of cell $(i-1, j)$.

In 1996, Sabeur *et al.*[22,23] implemented a weakly reflecting inflow boundary condition to model a wave generator. The discretised boundary condition is

$$u_{i-1,j}^{n+1} = u_{i-1,j}^{n} + \frac{\delta t \cdot C}{\delta x} \cdot (u_{i+1,j}^{n} - u_{i,j}^{n}) + \delta t \cdot H_u^n \tag{8}$$

$$v_{i-1,j}^{n+1} = v_{i-1,j}^{n} + \frac{\delta t \cdot C}{\delta x} \cdot (v_{i+1,j}^{n} - v_{i,j}^{n}) + \delta t \cdot H_v^n \tag{9}$$

and

$$\eta_{i-1,j}^{n+1} = \eta_{i-1,j}^{n} + \frac{\delta t \cdot C}{\delta x} \cdot (\eta_{i+1,j}^{n} - \eta_{i,j}^{n}) + \delta t \cdot E_u^n \tag{10}$$

where E and H are field operators of the water elevations and flow velocities from the right-hand side of the continuity equations at the inflow boundary, which are *a priori* known as an input. C is the computed wave celerity and is derived from the wave number k and wave period T

$$C = \frac{2\pi}{kT} \tag{11}$$

The field operators can be changed according to the type of wave implemented at the wave maker. In the case of random wave generation, the dispersion relation for progressive waves is no longer valid because of the wave number. In such circumstances, an input of experimental values of the wave number together with a listing of inflow velocity–time evolution must be implemented directly within the reflective boundary conditions.

This initial work was then followed by detailed simulations and comparisons with available experimental data, which are reported by Waller and Allsop.[24] This work included a dam break simulation and comparison with FLOW 3D, generation of regular waves in a rectangular basin, application to solitary waves, investigation of wave forces, run-up and overtopping on simple vertical and inclined walls, and comparison of the model output with data from an experimental flume. The program was then used to test the response and consistency of the numerical model to problems involving complex flows and geometries, as reported in Christakis *et al.*[25] and Waller *et al.*[26]

More recently, the Alternative Donor-Acceptor (ADA) scheme for fluid advection was developed and introduced in the model. In the classical Donor-Acceptor scheme, as described in Hirt and Nichols,[11] information both upstream and downstream of a free surface cell (i.e. a cell in the computational domain with at least one empty neighbour) is considered when calculating the fluid flux in and out of the cell, with the orientation of the fluid interface used to determine the amount of void present in a cell at each time-step. However, for the rest of the cells that contain fluid, only information upstream of a cell is used to determine the fluid fluxes during one model time-step. In this way, void 'bubbles' are entrapped within the fluid and are carried around with the flow, since the F function is considered homogeneously distributed within cells of the main fluid body. This clearly leads to loss of fluid momentum and a blurring of the fluid interface, due to the entrapped void regions. In the past, artificial numerical corrections have been applied to the calculated fluid flux between adjacent numerical cells to eliminate any void regions trapped within the fluid (see, for example, Torrey *et al.*[12]).

In the ADA scheme, the calculations of the directional gradients of the F function are extended to all cells containing fluid and not only at the free surface. Information both upstream and downstream of a cell is employed to determine a fluid interface orientation within all fluid cells. Hence, it becomes possible to calculate the total amount of void present within the fluid domain and priority is given to eliminating the void regions within the fluid body by first filling the upstream cells before fluid is allowed to enter downstream cells. As a result, the accuracy of pressure and velocity calculations is ensured, the loss of fluid momentum is minimised and a sharp fluid interface is maintained without the need of artificial numerical corrections.

Moreover, a third-order accurate upwind scheme, which considered one downwind and two upwind points, was also implemented in the model, for the discretisation in space of non-linear and diffusion terms in the finite difference operators A and B of equations (3), (4) and (5) away from free and solid boundaries; in this way, minimisation of numerical diffusion in the pressure and velocity calculations was achieved. The details of the differencing scheme can be found in Lemos.[27] The choice of this particular scheme was based upon its relatively simple treatment of solid and free boundaries and its requirement of fewer arithmetic operations per time-step, as compared to other higher-order differencing schemes.[27]

4. NUMERICAL SIMULATIONS AND TESTING OF NEWMOTICS-2D

A series of test simulations was performed to test the consistency of the model and its response to complex flows and geometries, as reported in Christakis *et al.*[25] and Waller *et al.*[26] A problem of great importance in engineering design studies was examined, notably a case of wave impact on a structure incorporating a horizontal deck. For this simulation, the model was set up with a flat bed and a sloping impermeable 1:2 structure leading to a horizontal deck. The deck was approximately 2 m long and 0·3 m thick. The distance between the open boundary and the toe of the structure was taken as 10 m and the mean water depth was 3 m; the still water level was initially approximately 1·5 m below the deck. A solitary wave of initial wave height of 1 m was assumed to enter the model at the open boundary at 0 s model time and propagated within 6·5 s up to the top of the slope. The results of this simulation are shown in Figs 2 and 3. As can be seen in Fig. 2, part of the wave crest hit and overtopped the deck, while the other part impacted on the underside of the deck.

Since there were no other similar data available to the authors to enable comparisons with the model output for water surface elevations and pressures, a check was made for the consistency of the model and its response to changes in the time-stepping. Fig. 3 shows the predicted pressure–time series during impact (between 6·3 and 6·4 s) for a cell on the underside of the deck, for different time-steps: Fig. 3(a) double the typical model time-

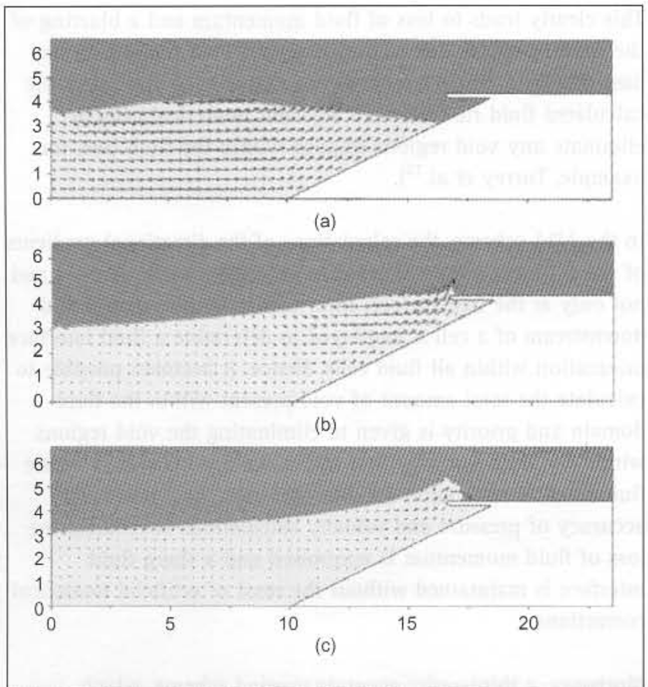

Fig. 2. Propagation of a solitary wave up a 1:2 sloping structure and impact with a horizontal deck. Free surface evolution at times: (a) 5 s; (b) 6·5 s; and (c) 7 s — wave height 1 m, still water depth 3 m, the arrows represent the velocity vectors

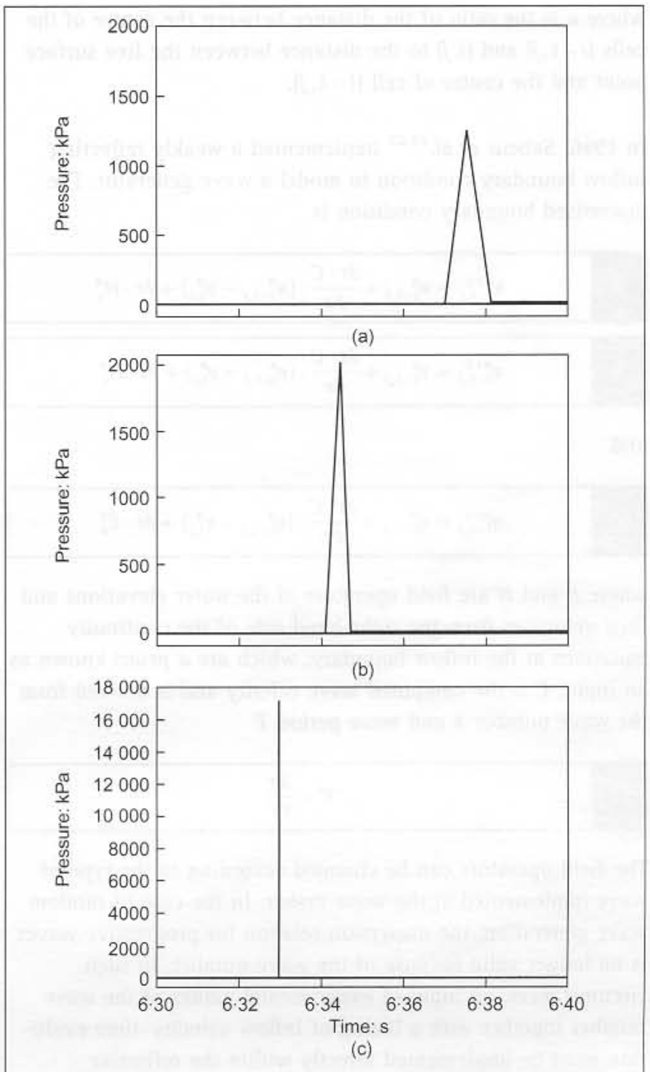

Fig. 3. Pressure–time series during impact for a single cell on the underside of the deck for different time-steps: (a) $2\delta t$; (b) δt; and (c) $\delta t/8$ ($\delta t \sim 10^{-2}$ s—typical model time-step)

step; Fig. 3(b) the typical model time-step; and Fig. 3(c) one eighth of the typical model time-step (a typical time-step, as calculated by the model, was of the order of 10^{-2} s). It was clear from this simulation that when the time-step was doubled (compare Figs 3(a) and 3(b)), the predicted maximum pressure was almost halved, with the impact extending over a longer period of time. In a similar manner, when the time-step was divided by eight (compare Figs 3(c) and 3(b)), pressure rose quite sharply to a maximum value almost eight times greater than before, with the impact pressure occurring almost instantaneously. However, the pressure impulse at impact (which results from time integration of the pressure) remained almost constant. This result is consistent with flow theory[28] and indicated the ability of the code to cope successfully with complex flow problems.

The performance of the combined ADA scheme/third-order upwind differencing scheme is demonstrated in a simple test simulation with a free-falling of a block of water in a tank, which impacts and merges with still water. The results are presented in Fig. 4, where a suspended 0·5 m × 0·5 m block of water with a hole at its centre is falling under gravity and impacting on still water in a 5 m × 3 m tank. A quite coarse grid size of 0·05 m in both the horizontal and the vertical was used. This demonstrates the ability of the ADA advection scheme to maintain the shape of the block during its free-fall (as expected theoretically) and to eliminate any void 'bubbles' from the main body of fluid after the impact and merging of the collapsing block with it. This can be seen clearly from the results presented in Fig. 4. It can be concluded that the newly developed ADA scheme constitutes a powerful algorithm for the advection of fluid between adjacent numerical cells. This simple numerical test illustrates the capability of the new scheme to maintain object shapes and sharp fluid interfaces without the need for artificial numerical corrections. Moreover, the grid size was chosen in order to demonstrate the numerical stability that the presented algorithm exhibits in quite coarse grids, thus making possible the minimisation of the total simulation run-time. It has also been stated that the new algorithm ensures the accuracy of pressure and velocity calculations and, thus, the minimisation of loss of fluid momentum. This will become especially clear in the sections that follow, where comparisons between numerical simulations and laboratory experiments are presented.

After the implementation and testing of the combined ADA scheme/higher-order differencing scheme, the numerical model was employed to simulate recent laboratory experiments carried out in an absorbing flume.[29] The flume was 40 m long, 1·5 m wide with an operating range of water depths at the wave paddle of 0·5–1·2 m. The piston paddle, which was driven by an electro-hydraulic system, was controlled by a computer, enabling either regular or random waves to be generated. Two wave probes mounted on the front face of the paddle measured the water surface elevation continuously.

Three main (impermeable) structure types were studied: 1:2 and

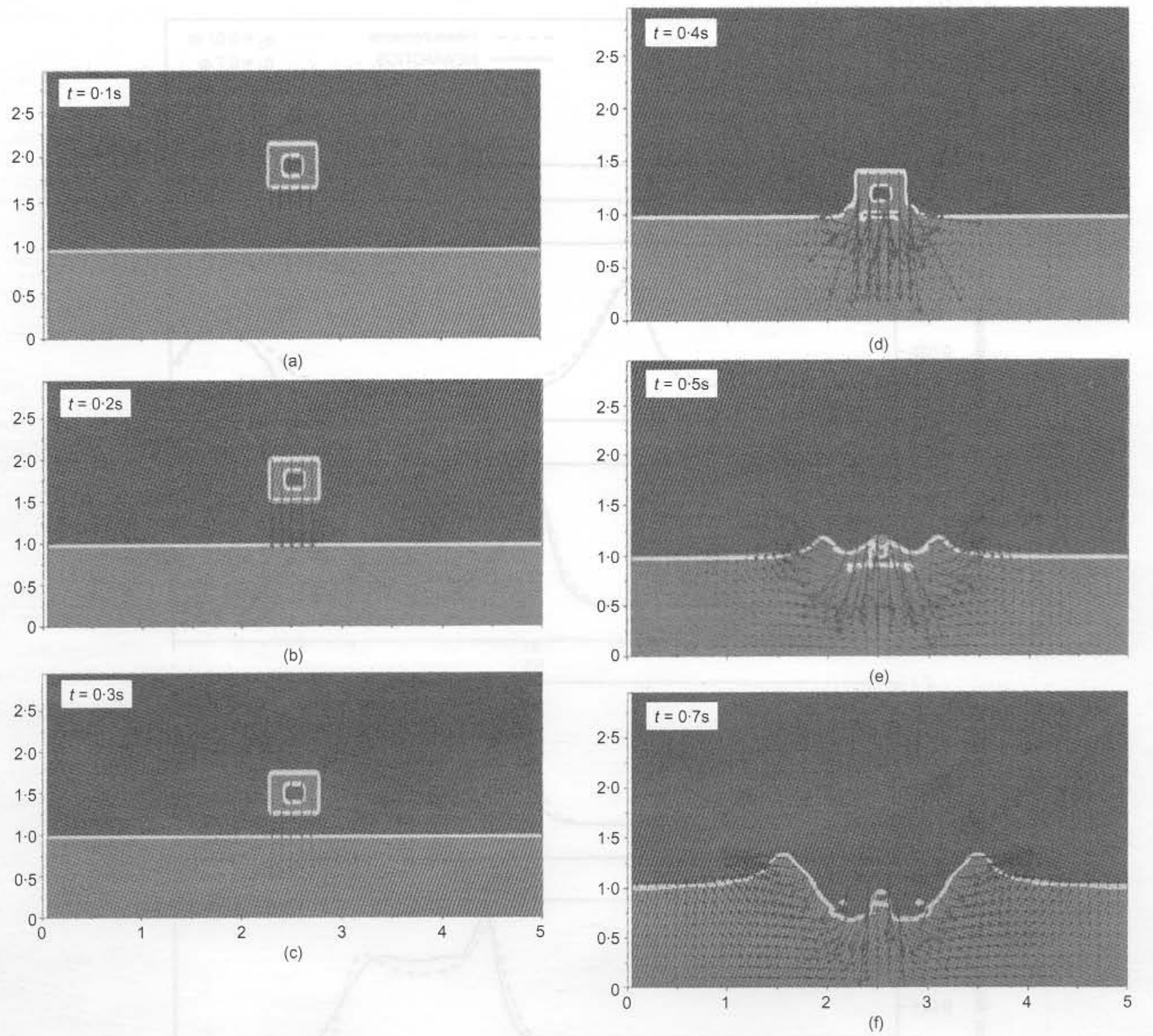

Fig. 4. Simulation of the free-fall under gravity of a suspended 0·5 m × 0·5 m block of water with a hole at its centre and impact on still water in a 5 m × 3 m tank—representation of the F function at different times; the arrows represent the velocity vectors; grid size $\Delta x = \Delta y = 0{\cdot}05$ m

1:4 smooth slope revetments, and a simple vertical wall. The responses of each structure were investigated using different bed slopes: 1:50, 1:20, 1:10 and 1:7. Each bed slope covered a vertical distance of 0·4 m from the flume floor to the toe of the structure, and so the horizontal lengths of the bed slopes ranged from 20 m for the 1:50 slope to 2·8 m for the 1:7 slope.

A number of twin wire probes were installed in order to measure water elevation time series at a frequency of 40 Hz. Their distances from the toe of the structure were 20 m, 10 m, 3·75 m, 3 m, 2·25 m, 1·5 m, 0·75 m and 0·5 m. Additionally, nine pressure transducers were positioned at different heights on the revetments and the simple vertical structure, which enabled the collection of pressure measurements of the wave at impact with the structures. The transducers were placed at different positions for different approach slopes.

For the numerical simulations, solitary wave datasets were chosen, because of their engineering importance, since they have the largest energy impulse and run-up, and consequently represent a good model for extreme design waves at coastal structures.[24] Each model run was set up to represent the flume from the toe of the bed slope upwards, since it was assumed that the solitary wave generated at the paddle was not modified before reaching the bed slope (see, for example, Waller *et al.*[26]). The inclined structures in the model were represented as a series of steps and particular attention was given to the choice of the grid dimensions, since sudden jumps in water depth, associated with the step representation, alter the wave characteristics if they are not performed carefully. Simulations were performed for selected cases of the two extreme approach slopes (1:50 and 1:7) and the numerical results were compared with the corresponding flume data, allowing for a 5% maximum uncertainty in the experimental measurements.[29] The 1:50 slope was chosen as indicative of all shallower slope angles. The steepest slope (i.e. 1:7), apart from the practical reason of having the smallest horizontal distance from the toe of the structure, was chosen as being indicative of shingle beaches.

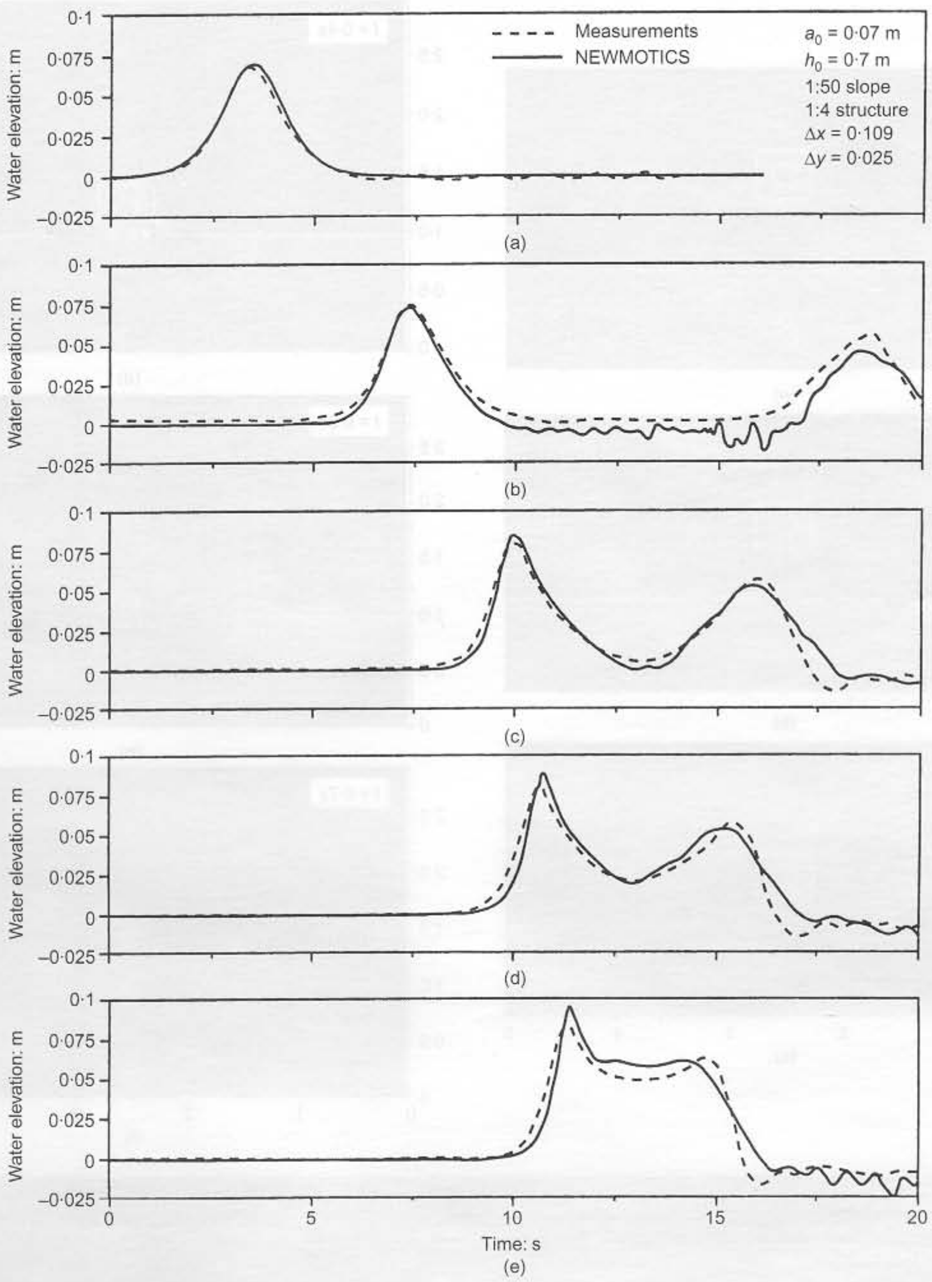

Fig. 5. NEWMOTICS-2D water elevation time series compared with measurements from an absorbing wave flume for various distances from the toe of the structure: (a) $x = -20{\cdot}00$ m; (b) $x = -10{\cdot}00$ m; (c) $x = -3{\cdot}75$ m; (d) $x = -2{\cdot}25$ m; and (e) $x = -0{\cdot}75$ m

In Fig. 5 the results of a simulation are presented where a solitary wave of height $a_0 = 0{\cdot}07$ m in still water depth $h_0 = 0{\cdot}7$ m runs up the 1:50 slope and impacts with a 1:4 structure. Water elevation time series predicted by the model are compared with experimental data obtained from the flume for different distances from the structure. Each separate graph corresponds to the time series of water elevation at a wave probe whose position is defined by its x coordinate relative to the toe of the structure. The dashed lines represent the flume measurements and the solid lines the model predictions. The grid size is 0·109 m and 0·025 m in the horizontal and the vertical, respectively. The numerical results were found to be in good agreement with the experimental data. Note that both the numerical simulations and the flume measurements show similar transformations of the initially symmetrical waves into asymmetrical waves as they propagate up the bed slope and the interactions between the incident and the reflected solitary waves appear to have been well represented by the numerical code.

The simulation was repeated for the same approach slope, structure and grid size but for different wave heights and still water depths ($a_0 = 0{\cdot}1$ m and $h_0 = 0{\cdot}5$ m, respectively). The results of these simulations are presented in Fig. 6, where water elevation time series from the model are compared with data from the flume for different distances from the toe of the structure. The dashed lines represent the flume measurements and the solid lines the model predictions. The numerical results were found to be in reasonable agreement with experimental data and it can be seen that the numerical model predicted the general pattern of the wave propagation. However, it was also observed that as the ratio of wave height to still water depth increased (in this case, this ratio was double the ratio of the

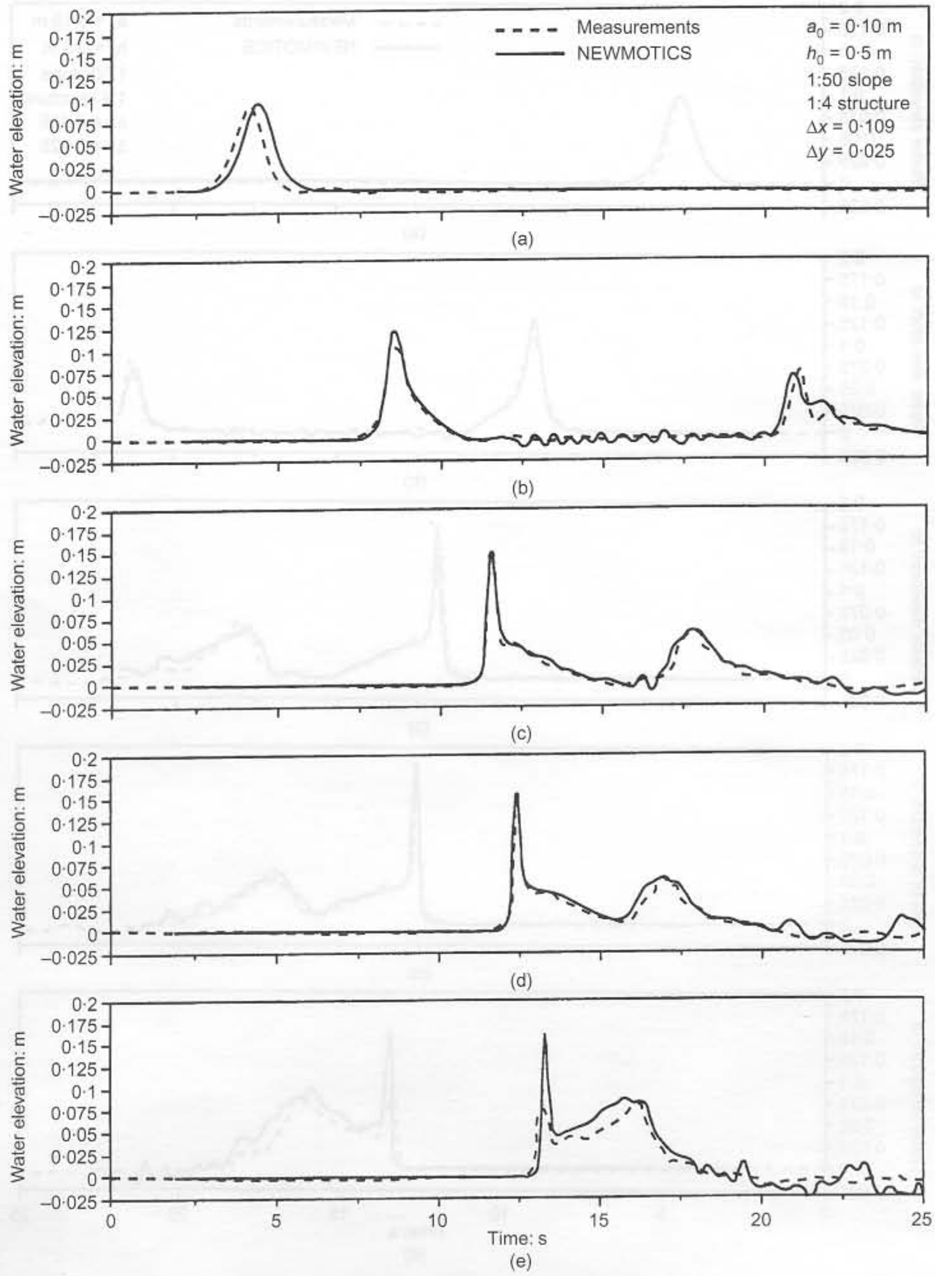

Fig. 6. NEWMOTICS-2D water elevation time series compared with measurements from an absorbing wave flume for various distances from the toe of the structure: (a) $x = -20{\cdot}00$ m; (b) $x = -10{\cdot}00$ m; (c) $x = -3{\cdot}75$ m; (d) $x = -2{\cdot}25$ m; and (e) $x = -0{\cdot}75$ m

previous simulation), the comparison between model and experiment deteriorated slightly, in particular, for measurements from probes positioned closer to the toe of the structure, where the interaction between incident and reflected waves occurs.

For this reason, the simulation of Fig. 6 was repeated with a finer grid. The grid size was reduced approximately by a half (0·055 m and 0·013 m in the horizontal and vertical, respectively) and the results are presented in Fig. 7. The dashed lines represent the flume measurements and the solid lines the numerical model predictions for water elevation time series for different distances from the toe of the structure. The numerical results for this case were found to be in a slightly better agreement with the flume data than in the case described in Fig. 6. Detailed root mean square (rms) values comparing the calculated time series water elevations with the experimental elevations are given in Table 1 for both time steps. It is notable that with the exception of the series at 20 m from the structure that there is very little difference implying that the coarse grid gives a good correlation with the experiments. The transformation of the wave from symmetrical to asymmetrical has been well represented by the model with the front face of the wave becoming steeper and the rear face less steep. In the light of these results, it may be argued that an almost inverse proportionality has been observed between the grid size and the ratio of wave height to still water depth. It has not been possible to verify this observation theoretically. However, it can be argued that a bigger wave height would cause the velocity of wave propagation (and thus, velocity of impact) to increase.[30] This would also lead to an increase of pressure at impact. In this case, to model the steeper pressure gradient

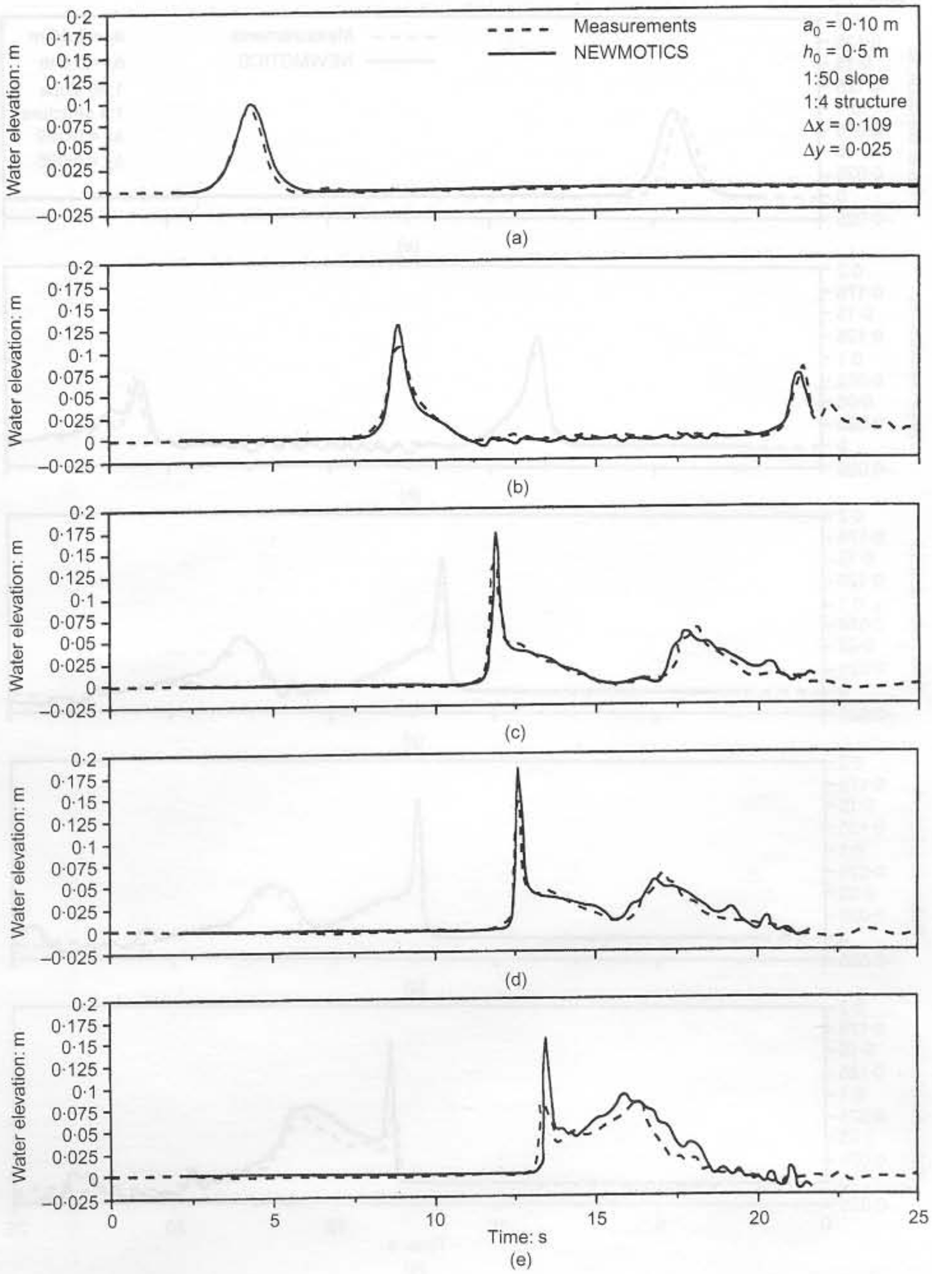

Fig. 7. NEWMOTICS-2D water elevation time series compared with measurements from an absorbing wave flume for various distances from the toe of the structure: (a) $x = -20.00$ m; (b) $x = -10.00$ m; (c) $x = -3.75$ m; (d) $x = -2.25$ m; and (e) $x = -0.75$ m

Distance from structure: m	Coarse grid: m	Fine grid: m
20·00	$8{\cdot}11 \times 10^{-3}$	$2{\cdot}28 \times 10^{-3}$
10·00	$5{\cdot}66 \times 10^{-3}$	$5{\cdot}68 \times 10^{-3}$
3·75	$4{\cdot}34 \times 10^{-3}$	$5{\cdot}43 \times 10^{-3}$
2·25	$5{\cdot}6 \times 10^{-3}$	$5{\cdot}49 \times 10^{-3}$
0·75	$1{\cdot}08 \times 10^{-2}$	$1{\cdot}04 \times 10^{-2}$

Table 1. Comparison between theory and experiment (rms values)

around impact time compared with the case of smaller wave height, would require a more refined grid, in order to achieve better convergence during the solution of the momentum equation in the numerical model and, thus, to represent correctly the effects of impact on the wave propagation.

For the simulation with the 1:7 approach slope a still water depth $h_0 = 0{\cdot}6$ m and a wave height $a_0 = 0{\cdot}1$ m were tested, and a vertical impermeable structure was chosen. Following the discussion from the previous section, concerning the ratio of wave height to still water depth, the grid was chosen as 0·08 m and 0·02 m in the horizontal and vertical directions, respectively. Pressures around the impact between the propagating wave and the vertical structure were calculated in front of the vertical wall at the corresponding transducer positions. A comparison between the numerical results and the experimental data from the flume is shown in Fig. 8. The dotted lines in this case correspond to the model output and the solid lines to the physical data from the flume for four different transducers, for which compressibility was not an issue. It can be seen that the numerical results from the model were in reasonable agreement with the flume experiments.

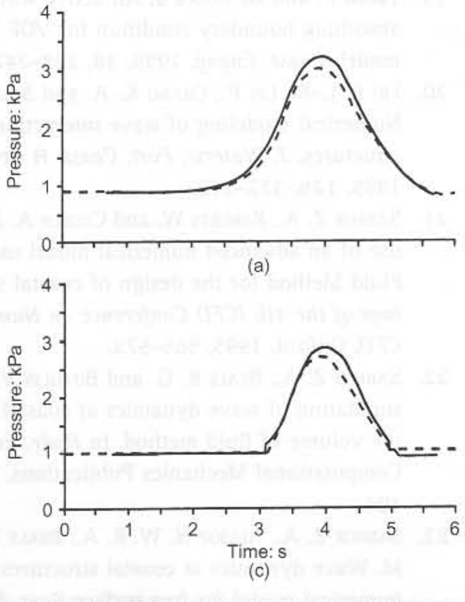

Fig. 8. NEWMOTICS-2D pressures at impact with vertical wall compared with measurements from an absorbing wave flume for four pressure transducers on the vertical structure. Height z corresponds to the distance of each transducer from the bed of the flume. Solitary wave case, 1:7 approach slope, vertical structure, wave height $a_0 = 0.1$ m, still water depth 0.6 m. Grid size $\Delta x = 0.08$ m, $\Delta y = 0.02$ m

5. DISCUSSION AND FUTURE DEVELOPMENTS OF NEWMOTICS-2D

Although the results from the numerical model are in agreement with the available experimental flume data, further developments of the program will be required. The program is currently only able to model flows around impermeable structures and does not include any turbulence models. Bracci-Laudiero[18] has shown, using an earlier version of the program, that flow in and around permeable structures can be included by modifying the governing Navier–Stokes equations. The influence of turbulence will be included in the next stage of development of the model. The program is currently relatively slow to solve flow problems on PCs, taking over 2 h for a single wave impact. The program will be speeded up by the addition of adaptive mesh techniques so that a fine discretisation is only required in regions modelling steep changes of velocities or pressure. The use of the ADA technique to improve modelling of, and to reduce diffusion of, the free surface is considered by the authors to be one of the most important developments of the program. Additional work will use techniques from fluid gas dynamics[31] to further improve fluid advection and free surface reconstruction. Despite the above limitations the model can currently simulate two-dimensional impermeable flows up to and around coastal structures, producing plots of fluid velocities and calculating pressures and pressure impulses on these structures.

6. CONCLUSIONS

The development and use of a new numerical model of wave dynamics, NEWMOTICS-2D based on the VOF technique, has been presented. The model has been shown to be capable of simulating complex flows and geometries. The incorporation of the ADA scheme for fluid advection has been discussed and its capability in minimising the loss of fluid momentum has been tested in conjunction with a third-order upwind differencing scheme. The model has been employed to simulate recent laboratory experiments carried out in an absorbing flume and it has been demonstrated that the model can successfully simulate the dynamics of waves at coastal structures, especially during the critical period of impact and breaking. This comparison with experimental data, for the type of model described, is believed to be unique. Thus, the program constitutes a powerful tool that will enable more detailed studies of wave-induced flows to be carried out by coastal and harbour engineers and hence improve the overall design process.

7. ACKNOWLEDGEMENTS

This work has been partially funded by the Department of Environment Construction Sponsorship Directorate under contract number CI 39/5/86, with some elements supported by contracts PECD 7/6/230, 7/6/107 and 7/6/108, and by Oxford Brookes University. The authors acknowledge the contributions made by Zoheir Sabeur, Xinyu He, Alberto Bracci-Lauderio, Martin Waller and Michael Turnbull to this project over the last seven years.

REFERENCES

1. Kobayashi N. and Raichle A.W. Irregular wave overtopping of revetments in surf zones. *J. Waterw. Port, Coast. & Ocean Engng*, ASCE, 1994, 120, 56–73.
2. Titov V. V. and Synolakis C. E. Modelling of breaking and nonbreaking long-wave evolution and run-up using VTCS-2. *J. Waterw. Port, Coast. & Ocean Engng*, ASCE, 1995, 121, 185–202.
3. Raubenheimer B., Guza R. T., Elgar S. E. and Kobayashi N. Swash on a gently sloping beach. *J. Geophys. Res.*, 1995, 100, 8751–8760.
4. Dodd N. Numerical model of wave run-up, overtopping and regeneration. *J. Waterw. Port, Coast. & Ocean Engng*, ASCE, 1998, 124, 73–81.
5. Maiti S. and Sen D. Computation of solitary waves during propagation and runup on a slope. *Ocean Engng*, 1999, 26, 1063–1083.

6. Yasuda T., Mutsuda H. and Mizutani N. Kinematics of overturning solitary waves and their relations to breaker types. *Coastal Engng*, 1997, 29, 317–346.
7. Grilli S. T., Svendson, I. A. and Subramaya R. Breaking criterion and characteristics for solitary waves on slopes. *J. Waterw. Port, Coast. & Ocean Engng*, ASCE, 1997, 123, 102–112.
8. Harlow F. H. and Welsh J. E. Numerical calculation of time-dependent viscous incompressible flow of fluid with free surface. *Physics of Fluids*, 1965, 8, 2182–2189.
9. Hotchkiss R. S. *Simulation of Tank Draining Phenomena with the NASA SOLA–VOF code.* Los Alamos National Laboratory, New Mexico, USA, 1979, Report No. LA-UR-3384.
10. Nichols B. D., Hirt C. W. and Hotchkiss R. S. *SOLA-VOF: A Solution Algorithm for Transient Fluid Flow with Multiple Free Boundaries.* Los Alamos National Laboratory, New Mexico, USA, 1980, Report No. LA-3385, UC-32 and UC-34.
11. Hirt C. W. and Nichols B. D. Volume of Fluid (VOF) method for the dynamics of free boundaries. *J. Comput. Phys*, 1981, 39, 201–225.
12. Torrey M. D., Cloutman L. D., Mjolsness R.C. and Hirt C. W. *A computer program for incompressible flows with free surfaces.* Los Alamos National Laboratory, New Mexico, USA, 1985, Report No. LA-10612-Ms.
13. Sicilian J. M., Hirt C. W. and Harper R. P. *Flow 3D: Computational Modelling Power for Scientists and Engineers.* Flow Science Inc, 1987, Report FSI 87–00–01.
14. Van der Meer J. W., Petit H. A. H., Van den Bosch P., Klopman G. and Broekens R. D. Numerical simulation of wave motion on and in coastal structures. *Proceedings of the 23rd International Conference on Coastal Engineering*, Venice, 1992, Vol. 2, pp. 1772–1784.
15. Petit H. A. H., Tonjes P., Van Gent M. R. A. and Van den Bosch P. Numerical simulation and validation of plunging breakers using a 2D Navier-Stokes model. *Proceedings of the 24th International Conference of the Coastal Engineering Research Council (ASCE)*, Kobe, 1994.
16. Bradford S. F. Numerical simulation of surf zone dynamics. *J. Waterw. Port, Coast. & Ocean Engng*, ASCE, 1994, 126, 1–13.
17. Van Gent M. R. A. and Petit H. A. H. Simulation of wave interaction with coastal structures. *Hydroinformatics '94*, Rotterdam, 1994, pp. 141–146.
18. Bracci Laudiero A. A bidimensional numerical model for the study of wave transmission inside permeable maritime structures. *Proceedings of the 28th Italian National Congress of Hydraulics and Hydraulic Structures*, Sept. 1998, 13 pp.
19. Troch P. and De Rouck J. An active wave generating-absorbing boundary condition for VOF type numerical model. *Coast. Engng*, 1999, 38, 223–247.
20. Liu P. L.-F., Lin P., Chang K.-A. and Sakakiyama T. Numerical modeling of wave interaction with porous structures. *J. Waterw. Port, Coast. & Ocean Engng*, ASCE, 1999, 125, 322–330.
21. Sabeur Z. A., Roberts W. and Cooper A. J. Development and use of an advanced numerical model using the Volume of Fluid Method for the design of coastal structures. *Proceedings of the 4th ICFD Conference on Numerical Methods in CFD*, Oxford, 1995, 565–573.
22. Sabeur Z. A., Beale R. G. and Bovolin V. A full numerical simulation of wave dynamics at coastal structures with the volume of fluid method. In *Hydr. Eng. Soft. VI*, Computational Mechanics Publications, 1996, pp. 395–404.
23. Sabeur Z. A., Allsop N. W. R. A., Beale R. G. and Dennis J. M. Wave dynamics at coastal structures: development of a numerical model for free surface flow. *Proceedings of the 25th International Conference of the Coastal Engineering Research Council*, Orlando, 1996, pp. 389–402.
24. Waller M. N. H. and Allsop N. W. H. *Wave dynamics at coastal structures: development of numerical modelling methods.* HR Wallingford, 1997, Hydraulics Research Report SR496.
25. Christakis N., Waller M. N. H., Beale R. G. and Dennis J. M. The application of the volume of fluid method to wave dynamics at impermeable coastal structures. In *Numerical Methods for Fluid Dynamics VI*, Oxford, 1998, pp. 269–276.
26. Waller M. N. H., Christakis N., Allsop N. W. H., Beale R. G. and Dennis J. M. Development and validation of a numerical model of wave dynamics. *Proceedings of the 17th International Conference on Offshore Mechanics and Arctic Engineering*, Lisbon, 1998, Paper OMAE98–4086.
27. Lemos C. M. Higher-order schemes for free surface flows with arbitrary configurations. *Int. J. Numer. Methods Fluids*, 1996, 23, 546–566.
28. Okamura M. The pressure impulse distribution due to wave impact on a vertical plane wall. *J. Phys. Soc. Japan*, 1993, 62, 2285–2292.
29. Coates T., Jones R. J. and Bona P. F. D. Wind/swell seas and steep approach slopes: Report on wave flume studies. HR Wallingford, 1997, Hydraulics Research Report TR 24
30. Faber T. E. *Fluid dynamics for physicists.* Cambridge University Press, Cambridge, 1997.
31. Rider W. J. and Kothe D. B. Reconstructing volume tracking. *J. Comput. Phys.*, 1998, 141, 112–152.

Please email, fax or post your discussion contributions to the secretary by 1 March 2003: email: lyn.richards@ice.org.uk; fax: +44 (0)20 7799 1325; or post to Lyn Richards, Journals Department, Institution of Civil Engineers, 1–7 Great George Street, London SW1P 3AA.